JOC The Journal of Organic Chemistry

Article

pubs.acs.org/joc

Reaction of Nitrosonium Cation with Resorc[4]arenes Activated by Supramolecular Control: Covalent Bond Formation

Francesca Ghirga,[†] Ilaria D'Acquarica,*[,†] Giuliano Delle Monache,[†] Luisa Mannina,[†] Carmela Molinaro,[†] Laura Nevola,[†,‡] Anatoly P. Sobolev,[§] Marco Pierini,*[,†] and Bruno Botta[†]

[†]Dipartimento di Chimica e Tecnologie del Farmaco, Sapienza Università di Roma, P. le Aldo Moro 5, 00185 Roma, Italy

[§]Laboratorio di Risonanza Magnetica "Annalaura Segre", Istituto di Metodologie Chimiche CNR Area della Ricerca di Roma, Via Salaria km 29.300, 00015 Monterotondo, Italy

Supporting Information

ABSTRACT: Resorc[4]arenes **1** and **2**, which previously proved to entrap NO^+ cation within their cavities under conditions of host-to-guest excess, were treated with a 10-fold excess of $NOBF_4$ salt in chloroform. Kinetic and spectral UV−visible analyses revealed the formation of isomeric 1:2 complexes as a direct evolution of the previously observed event. Accordingly, three-body **1**−$(NO^+)_2$ and **2**−$(NO^+)_2$ adducts were built by MM and fully optimized by DFT calculations at the B3LYP/6-31G(d) level of theory. Notably, covalent nitration products **4**, **5** and **6**, **7** were obtained by reaction of $NOBF_4$ salt with host **1** and **2**, respectively, involving macrocycle ring-opening and insertion of a nitro group in one of the four aromatic rings. In particular, compounds **4** and **6**, both containing a trans-double bond in the place of the methine bridge, were oxidized to aldehydes **5** and **7**, respectively, after addition of water to the reaction mixture. Calculation of the charge and frontier orbitals of the aromatic donor (HOMO) and the NO^+ acceptor (LUMO) clearly suggests an ipso electrophilic attack by a first NO^+ unit on the resorcinol ring, mediated by the second NO^+ unit.

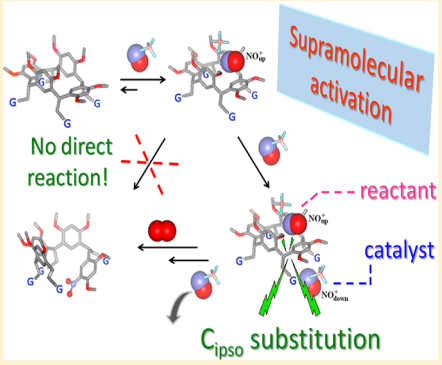

INTRODUCTION

C-Nitroso compounds participate in various biological processes: alkyl nitrites (RO−NO), nitrosoamines/amides, organic nitrates, and nitrosothiols are used in medicine as NO-releasing drugs,[1−5] whereas toxic NO_X gases, including NO, N_2O_3, NO_2/N_2O_4, and N_2O_5 may produce mutagenic nitrosoamines/peptides and may nitrosate and deaminate DNA as well.[6−9] Nitrosonium cation (NO^+), a close relative of NO, is known to insert into metal complexes to give metal−nitrosyl systems,[10] and to react with calixarene platforms by forming very stable host−guest complexes, both in solution and in solid state.[11−15] Such calixarene-based systems are now considered as supramolecular materials for generation, detection, storage, and release of NO.[16,17]

We previously reported that resorc[4]arene octamethyl ethers **1**, **2**, and **3** (Chart 1), when treated with $NOBF_4$ salt in chloroform, entrap highly reactive NO^+ species within their cavities.[18] The complexation process is proved by bathochromic shifts of the UV absorbance and is reversible: addition of water or alcohols leads in all cases to dissociation of the NO^+ complexes and to a complete recovery of empty resorc[4]-arenes. Stable 1:1 resorcarene−nitrosonium complexes of **1**−**3** were quantitatively isolated and fully characterized, using at least a 10-fold excess of host to guest. Under the same conditions, we also evaluated the role played by different side chains in the resorc[4]arene hosts (**1** vs **2**) and conformations (**2** vs **3**) for NO^+ encapsulation by an integrated analysis of spectral, kinetic, and molecular modeling data.[18] We now report the results obtained when resorc[4]arenes **1** and **2** were treated with excess $NOBF_4$ salt (up to 10-fold).

Chart 1. Resorc[4]arenes Studied as Hosts for Nitrosonium Cation (NO^+) Guest

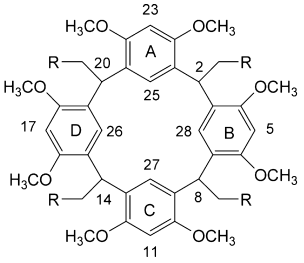

R
1 CH_2Br (*cone*)
2 COOEt (*cone*)
3 COOEt (*chair*)

RESULTS AND DISCUSSION

Complexation of calix[4]arenes by NO^+ cation under conditions of guest-to-host excess, as reported in the literature, may generate either complexes with stoichiometry greater than 1:1[12] or covalent side products.[19] In a previous work,[18] based on monitoring the UV−visible spectra of resorc[4]arene/NO^+ mixtures as a function of time, we found significant differences in the corresponding kinetic profiles when the host/guest ratio had been changed from 10:1 to 1:≥3. With the aim to clarify

Received: March 28, 2013
Published: June 20, 2013

   dx.doi.org/10.1021/jo400489m | *J. Org. Chem.* 2013, 78, 6935−6946

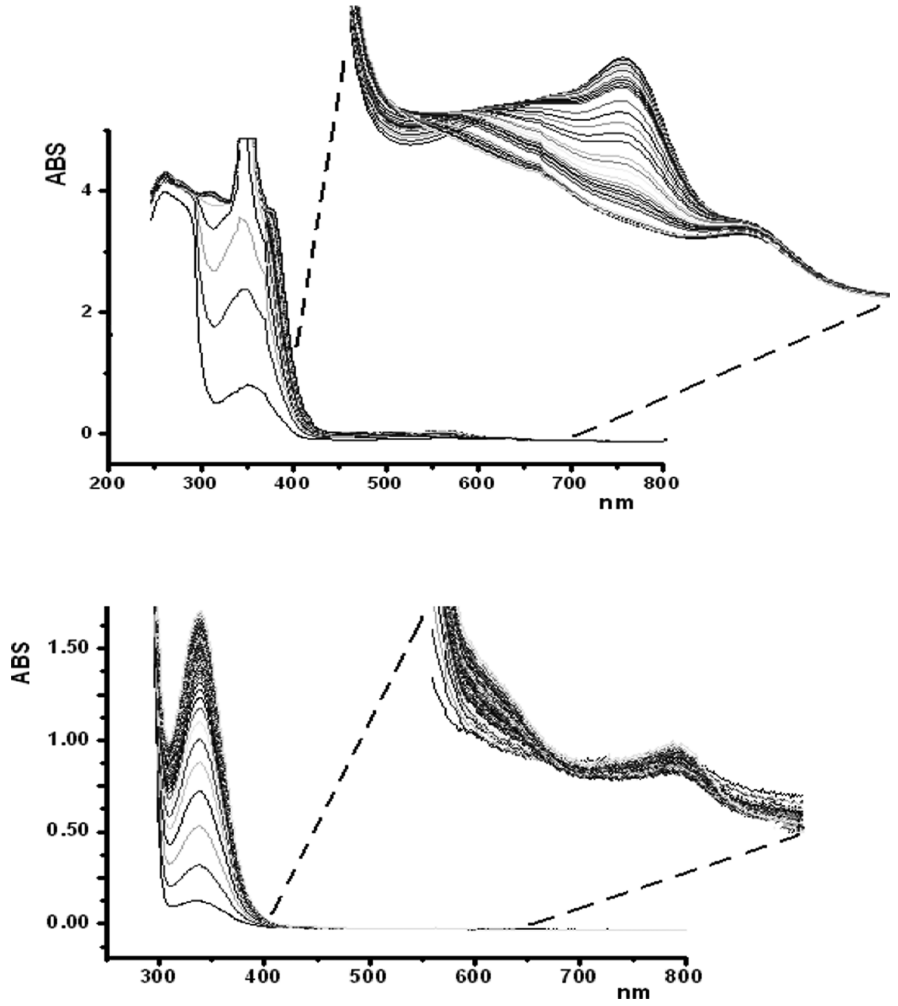

Figure 1. Spectrophotometric changes for the reactions between resorc[4]arene **1** (top) and resorc[4]arene **2** (bottom) with $NOBF_4$ salt in $CHCl_3$ (molar ratios 1:10) at 298 K.

the role played by the NO^+ cation in the interaction with resorc[4]arenes, we carried out accurate experiments involving spectral, kinetic, chromatographic, and molecular modeling measurements.

Because we demonstrated the prominent role played by the nature of the resorcarene substituents in the complexation, with respect to conformation,[18] we directed our attention to resorc[4]arenes **1** and **2**, which share the same cone conformation but feature different side chains (see Chart 1). To figure out all the possible phenomena involved, resorc[4]-arenes **1** and **2** were treated with an excess of NO^+ cation (from a saturated chloroform solution of $NOBF_4$ salt), and the rate of absorption changes of the resultant solutions were monitored in the 300−800 UV−visible nm wavelength range at 298 K. As compared with the spectra of the same resorc[4]arenes treated with a host-to-guest excess,[18] the UV−visible absorptions in the low-energy bands (LEB) were drastically reduced and appeared only by a strong magnification (Figure 1), whereas the growth of the absorptions in the high-energy bands (HEB) zone took place faster.

Kinetic Studies on Resorc[4]arene 1. The kinetic pathway for the formation of **1**−NO^+ complexes was monitored under pseudo-first-order conditions, recording in the 250−800 nm UV−visible wavelength range spectra of chloroform solutions containing a guest-to-host molar ratio equal to 10. Two bands at λ_{max} = 561 and 626 nm (LEB zone), after a fast initial growth, gradually decreased to achieve a minimum at both wavelengths (Figure 2). A bit slower growth was recorded at the wavelength range from 250 to 340 nm. The shape of the growing spectral bands in the visible zone closely resembles the analogous process already observed when preliminary experiments were carried out under conditions of **1** to NO^+ excess, which was rationalized as due to three consecutive steps (denoted as steps I, II, and III).[18] This phenomenon at that time was attributed to the quick generation of a **1**/NO^+ adduct of 1:1 stoichiometry, with the nitrosonium cation located inside the cone cavity of the resorcarene host (namely, the **1*a***−NO^+ structure), which next undergoes a slower evolution (a true first-order kinetics) toward a new isomeric form of the complex (the **1*b***−NO^+ adducts[18]). However, differently from that behavior, in the present study, after the analogous initial growth of the absorption bands in the LEB zone, a rapid stop followed by a progressive decrease of their intensities was detected. These observations suggest that, after the formation of the above 1:1 host−guest adduct (with NO^+ inside the cone cavity), a new supramolecular species, activated to undergo a spontaneous intramolecular modification (reasonably a complex with a 1:2 host−guest stoichiometry), arises from the first. The emergence of this species is indirectly monitored by the isosbestic point at

dx.doi.org/10.1021/jo400489m | J. Org. Chem. 2013, 78, 6935−6946

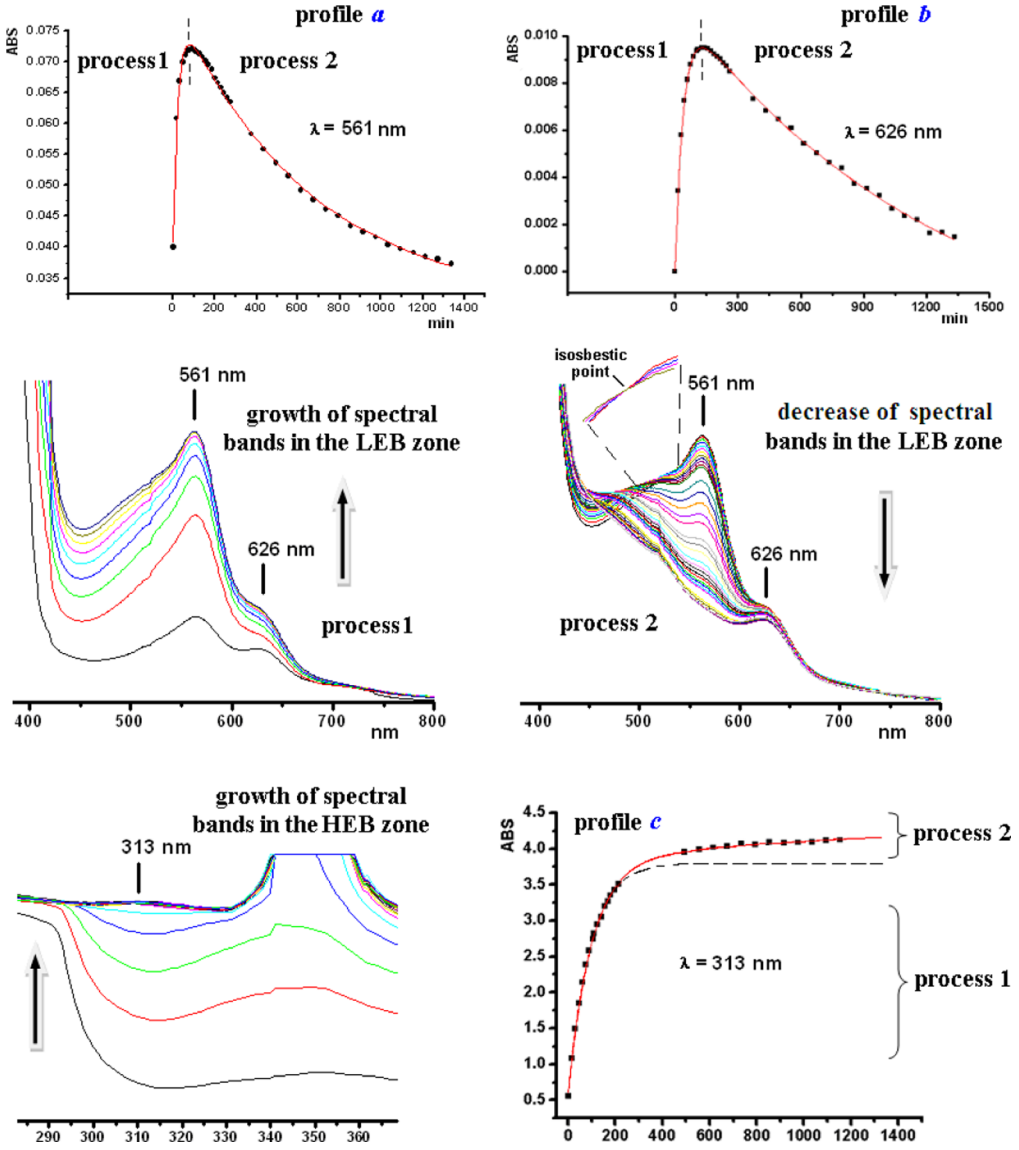

Figure 2. Kinetic pathway of the interaction between resorc[4]arene **1** and NO^+ cation monitored by UV spectroscopy in the LEB (λ = 561 and 626 nm) and in the HEB (λ = 313 nm) zones.

Table 1. First-Order Rate Constants (s^{-1}) for the Interaction of Resorc[4]arenes 1 and 2 with Excess Added $NOBF_4$ Salt[a]

host	host concn (M)	$NOBF_4$ concn (M)	kinetic event	λ = 313 nm	λ = 626 nm	λ = 339 nm	λ = 563 nm
1	2.7×10^{-3}	2.5×10^{-2}	process 1	1.8×10^{-4}	4.2×10^{-4}	–	–
			process 2	1.2×10^{-5}	1.3×10^{-5}	–	–
	1.0×10^{-3}	2.5×10^{-2}	process 1	–	6.2×10^{-4}	–	–
			process 2	–	–	–	–
2	5.3×10^{-4}	5.6×10^{-3}	process 1	–	–	9.2×10^{-4}	2.2×10^{-4}
			process 2	–	–	1.5×10^{-6}	1.5×10^{-6}

[a]Plots of the corresponding kinetic pathways (spectral changes as a function of time) are collected in Figures 2 and 6.

503 nm, visible in Figure 2. The next changes suffered by the new hypothesized adduct would be, in fact, responsible for the triggered loss of absorbance in the LEB zone. In other words, the whole evolution of the spectral absorptions in the visible zone would be the result of connected and partially superimposed processes of supramolecular (in the first stage) and covalent (in the next step) origin. The spectral changes, collected as a function of time in the LEB zone, were processed by nonlinear curve-fitting analysis according to a couple of partially superimposed first-order processes (kinetic events 1 and 2 in Figure 2 and Table 1) and afforded good correlation coefficients (in all cases >0.99). Nonlinear curve fitting was also carried out on the spectral changes registered in the HEB zone (λ_{max} = 313 nm, see Table 1), which are again connected to two consecutive processes, featuring very different rates (namely, processes 1 and 2 of profile c in Figure 2). Again, according to our previous results,[18] the faster process (namely, process 1, λ = 313 nm, $k_1 = 1.8 \times 10^{-4}$ s^{-1}) should be associated with the

dx.doi.org/10.1021/jo400489m | J. Org. Chem. 2013, 78, 6935−6946

coordination of a NO^+ guest unit under the convex side of the resorcarene *lower rim* defined by the side-chain substituents. In principle, this insertion might involve either uncomplexed host **1** (a process that leads to the **1c**−NO^+ geometry discussed in ref 18 and here reconsidered in the performed theoretical approach, see Figure 3) or an already *upper rim*-complexed host

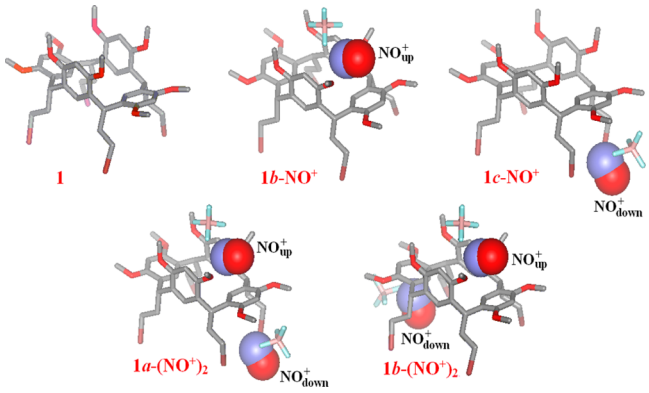

Figure 3. Structures obtained by DFT calculations for resorc[4]arene **1** and its two-body (**1b**−NO^+ and **1c**−NO^+) and three-body (**1a**−$(NO^+)_2$ and (**1b**−$(NO^+)_2$) adducts with NO^+ cation (the counterion BF_4^- was added to keep neutral the supermolecules).

(i.e., the **1b**−NO^+ structure), which would lead to three-body adducts such as those depicted in the bottom of Figure 3 (vide infra). However, the large excess of NO^+ cation used with respect to the corresponding formation of **1c**−NO^+ adducts[18] preferentially account for a complex with a 1:2 host−guest stoichiometry.

Accordingly, the second and slower event (namely, process 2, λ = 313 nm, $k_1 = 1.2 \times 10^{-5}$ s^{-1}), that was not detected at all in host-to-guest excess conditions, takes place with a rate virtually indistinguishable from that measured by the spectral changes in the LEB zone (i.e., process 2, λ = 626 nm, $k_1 = 1.3 \times 10^{-5}$ s^{-1}). Its linear kinetic profile, therefore, is consistent with the hypothesized initial stage of a first-order transformation leading to a product that is forming, which is devoid in its visible spectra of the absorption band at 561 nm. Finally, a much stronger absorption, running off-scale, was also registered in the 340−360 nm range (see Figure 2), exactly the UV zone corresponding to the electron transitions for the NO^+ species.

To summarize, after than a first NO^+ unit has been accommodated into the cone cavity of resorc[4]arene **1** (a process that is allowed by the optimization of NO^+−aromatic charge-transfer interactions[18]); a second NO^+ unit is encapsulated within the lower rim of the host, leading to the above 1:2 complex that, in turn, is ready to undergo a spontaneous monomolecular modification. Such a process, that in principle could be either supramolecular or covalent, is evoked by a clear isosbestic point centered at 503 nm (Figure 2). To provide additional information on the species detected, several experiments featuring changes in the reaction time and in the [**1**]/[NO^+] molar ratio were performed. Periodic monitoring of the reaction mixtures was carried out by both NMR and HPLC techniques, before and after the quenching of the chloroform solutions with water. Notably, upon addition of water, the solutions bleached (from deep purple to pale yellow), as under conditions of host excess,[18] but as the [**1**]/[NO^+] molar ratios changed from 1:1 to 1:3, the NMR spectra showed the appearance of new signal resonances, beside those belonging to the starting resorcarene. The bleached solutions were thus analyzed by normal-phase (NP) HPLC (for experimental conditions, see the Supporting Information). Figure 1S of the Supporting Information shows the chromatograms obtained after bleaching of **1**/NO^+ mixtures at 1:1, 1:2, and 1:3 molar ratios. When bleached solutions from **1**/NO^+ = 1:1 mixtures were examined, the parent resorc[4]arene **1** was recovered almost exclusively (peak A, 90%), as in previous experiments with host excess.[18] However, upon increasing the NO^+ concentration, two new products (peaks B and C, 60−80%) were formed at the expense of the parent resorc[4]arene (40−20%). Compounds **4** and **5** (corresponding to peaks B and C, respectively) were first isolated by preparative TLC, checked for purity by NP-HPLC (85−90%), and then fully characterized by both 1D and 2D NMR techniques (HMBC, HSQC, and TOCSY). Electrospray ionization−high resolution mass spectrometry (ESI-HRMS) was used to complete identification of compound **5** (see the Supporting Information), while elemental analysis was performed for compound **4**.

Identification of Compounds 4 and 5 by NMR Spectroscopy. ^1H NMR spectra of the new compounds exhibited several signals for the aromatic protons (one for each proton) instead of the two signals (one for type, Hi or He, of proton) given by the parent resorc[4]arene **1**. The same happened for the eight singlet signals of the methoxyl groups (only one signal in the precursor). Notably, whereas the He signals (i.e., H-5, H-11, H-17, and H-23, see Chart 1) appeared approximately in the same region for the two compounds, the Hi signals (i.e., H-25, H-26, H-27, and H-28) were shifted downfield, as compared with those of **1**. Moreover, only the signals for three bridge methines and relative substituents were observed. In the ^1H spectrum of **4**, the doublet signals of two coupled (J = 15.7 Hz) trans-olefinic protons (at δ = 6.81 and 6.21 ppm) and the appearance of a bromoethyl group suggested the presence of a HC═CH−CH_2Br system, while in the spectrum of **5** a new singlet at δ = 10.24 ppm was attributed to an aldehyde group. Cumulatively, these findings suggest for compounds **4** and **5** a rupture of one of the methine bridges (e.g., C-2, see Chart 1) that leads to the loss of the C_{4v} symmetry of the cone conformation and to the plurality of signals. As a result, the methine and its substituent are converted to a 3-bromopropylene group in compound **4** and oxidized to CHO in compound **5** (see Chart 2).

To understand the destiny of carbons 1 and 3 (see Chart 1), we may consider that the above-mentioned downfield shifts, caused by the loss of the deshielding due to the opponent aromatic nucleus, were not comparable for the Hi protons: two of them, indeed, reached the very high values of 7.15 (H-25) and 7.79 (H-28) ppm in compound **4**, and 7.60 and 7.75 ppm

Chart 2. Structures of Compounds 4 and 5 Obtained from Resorc[4]arene 1

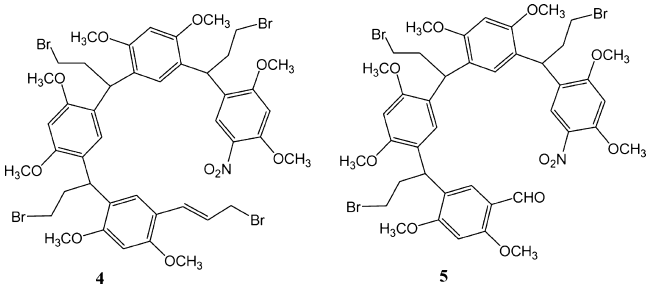

dx.doi.org/10.1021/jo400489m | J. Org. Chem. 2013, 78, 6935−6946

Table 2. Charge and Frontier Orbital Properties Calculated for Uncomplexed Resorc[4]arenes 1 and 2 and for Their Two-Body and Three-Body Adducts with NO^+ Cation

			charge on N atoms (electrons)		charge on C_{ortho} and C_{ipso} atoms (electrons)				LUMO−HOMO gap (eV)	
					close to NO^+_{up}		close to NO^+_{down}			
host or NO^+ adduct	relative stability (kcal mol^{-1})	BP[a] (%) at 298 K	NO^+_{up}	NO^+_{down}	C_{ortho}	C_{ipso}	C_{ortho}	C_{ipso}	NO^+_{up}	NO^+_{down}
1	–	–	0.205[b]		−0.192	−0.087	–	–	2.4[b]	
1b−NO^+	0.0	100.0	0.562	–	−0.197	−0.087	–	–	1.4	–
1c−NO^+	6.4	0.0	–	0.520	–	–	−0.205	−0.086	–	0.7
1a−$(NO^+)_2$	8.5	0.0	0.569	0.530	−0.208	−0.092	−0.208	−0.092	1.2	0.7
1b−$(NO^+)_2$	0.0	100.0	0.570	0.402	−0.198	−0.088	−0.209	−0.040	1.3	2.8
2	–	–	0.205[b]		−0.173	−0.075	–	–	1.9[b]	
2b−NO^+	4.4	0.1	0.561	–	−0.197	−0.087	–	–	1.2	–
2c−NO^+	0.0	99.9	–	0.639	–	–	−0.196	−0.091	–	0.9
2a−$(NO^+)_2$	0.0	69.9	0.567	0.639	−0.200	−0.097	−0.200	−0.097	1.3	1.1
2b−$(NO^+)_2$	0.5	30.1	0.565	0.628	−0.198	−0.091	−0.200	−0.088	1.2	1.1

[a]BP = Boltzmann population. [b]Data obtained from uncomplexed NO^+ cation (i.e., $NOBF_4$).

in compound **5**. This can be explained for the H-25 proton by the proximity of the double bond (in compound **4**) or the aldehyde group (in compound **5**), whereas for the second (H-28) we have to invoke the presence of an ortho polar group, such as OH, but more reasonably NO or NO_2, in C-3. Accordingly, two of the eight quaternary aromatic carbons are shifted in the ^{13}C NMR spectra upfield (δ = 116.5 ppm) and downfield (δ = 131.8 ppm) with respect to the parent resorc[4]arene **1** and were attributed to C-1 and C-3, respectively. The presence of a NO_2 group attached to an aromatic ring was confirmed by the two typical absorption bands caused by symmetrical and asymmetrical stretching vibrations of the N═O double bond at 1330−1299 and 1500−1465 cm^{-1}, respectively, found in the Fourier transform infrared spectra of compounds **4** and **5**.

The structures **4** and **5** (Chart 2) were assigned to the two products. The above results suggested that at least two events may be responsible for the macrocycle ring-opening: (i) an aromatic protodealkylation reaction, frequently observed for alkyl-substituted aromatic compounds in the presence of strong Lewis acids,[20,21] and (ii) an ipso electrophilic aromatic substitution (S_EAr) by NO^+.[22]

In summary, isolation of compounds **4** and **5** from resorc[4]arene **1** showed that, depending on the concentration, NO^+ cation could behave, at the same time, as reactant and catalyst. The former behavior is demonstrated by the presence, in both the two products, of the nitro group (the end oxidation product of the nitroso substituent) in one of the four aromatic rings. The second performance is suggested by the fact that compounds **4** and **5** could be obtained only when $[NO^+]/[\mathbf{1}]$ molar ratios were ≥1, whereas only complexation phenomena could take place for molar ratios ≤1. Thus, we may suppose an ipso electrophilic attack by a second unit of NO^+ on the resorcinol dimethyl ether ring, catalyzed by an already hosted NO^+ cation (vide infra).

Because both polar and radical processes involving the NO^+ cation as the reactive species have been reported in the literature,[21] we checked the nature of our transformation by adding hydroquinone and benzophenone separately to the resorcarene/NO^+ mixtures. No relevant changes were detected when the reaction was carried out in the presence of such radical scavengers. To explore the feasibility of the mechanism leading to compounds **4** and **5** from resorc[4]arene **1**, we set up several experiments followed by classical molecular modeling calculations.

Molecular Modeling Studies on Resorc[4]arene 1. The starting points of our theoretical calculations were the **1b**−NO^+ and **1c**−NO^+ geometries obtained from previous studies on **1**−NO^+ complexes under conditions of host excess[18] (see Figure 3). Under conditions of guest excess, we may suppose that a second NO^+ unit further interacts, preferably in the nitrosonium cation-free regions, either in the upper or in the lower rim of already formed **1x**−NO^+ complexes (with **x** = **b** or **c**). According to that, three-body adducts have been modeled, considering also the presence of the counterion (BF_4^-), by adding a new NO^+ cation inside the cone cavity of the **1c**−NO^+ two-body adduct, obtaining two different geometries, namely **1a**−$(NO^+)_2$ and **1b**−$(NO^+)_2$ (Figure 3). Afterward, the two geometries were first fully optimized by ab initio Hartree−Fock (HF) calculations and next refined by the density functional theory (DFT) method at the B3LYP/6-31G(d) level of theory. Geometry **1b**−$(NO^+)_2$ proved to be more stable than **1a**−$(NO^+)_2$ by 8.5 kcal mol^{-1} at 298 K (see Table 2); therefore, calculation of Boltzmann populations in the gas phase suggests that the amount of complex **1a**−$(NO^+)_2$ is negligible at 298 K. In both of the three-body complexes, the nitrogen of the cation accommodated inside the cone cavity (namely, NO^+_{up}) is pointing toward a *flattened* aromatic ring, with its van der Waals sphere almost in contact with those of both the aromatic carbons bound to the methine bridges (namely C_{ipso} atoms, see Figure 4), the distance N−C_{ipso} being 3.62 Å in **1a**−$(NO^+)_2$ and 3.79 Å in **1b**−$(NO^+)_2$. The same holds for the van der Waals sphere of the carbon atom which is ortho to the couple of C_{ipso} atoms (namely C_{ortho}, see Figure 4), the distance N−C_{ortho} being 3.50 Å in **1a**−$(NO^+)_2$ and 3.67 Å in **1b**−$(NO^+)_2$. However, only in **1b**−$(NO^+)_2$ geometry the second NO^+ unit placed in the lower rim of the resorcarene (NO^+_{down}) and pointing its nitrogen atom toward the center of a flattened aromatic ring displays this atom at a very short distance from the C_{ipso} and the C_{ortho} carbon atoms, even shorter than that found for NO^+_{up} (see Figure 4). N−C_{ipso} and N−C_{ortho} distances of 4.91 Å and 4.90 Å were, in fact, measured for **1a**−$(NO^+)_2$, respectively, while for **1b**−$(NO^+)_2$, they were 2.55 Å and 2.47 Å. The tight atomic contacts measured for both of the NO^+ units in **1b**−$(NO^+)_2$ geometry strongly suggests, by entropic factors, that either the NO^+ cation inside the cone cavity or that located outside the macrocycle and leaning

dx.doi.org/10.1021/jo400489m | J. Org. Chem. 2013, 78, 6935−6946

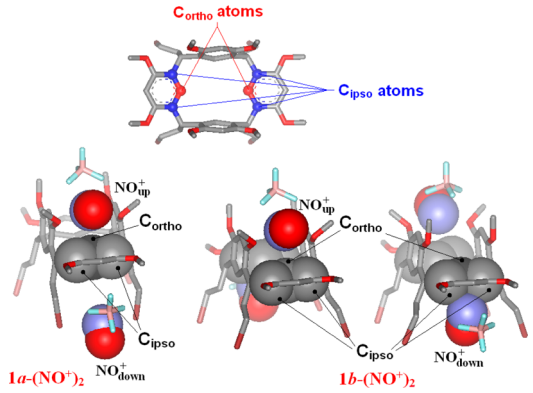

Figure 4. Calculated proximity of the nitrogen atom of NO^+ cation units with C_{ipso} and C_{ortho} carbon atoms of resorc[4]arene **1** in three-body **1a**$-(NO^+)_2$ and **1b**$-(NO^+)_2$ adducts.

against one aromatic ring may easily trigger a classical electrophilic aromatic substitution (S_EAr) on the resorcinol dimethyl ether ring.

To give a quantitative support to the picture, we evaluated the charge and frontier orbital properties of the aromatic donor (HOMO) and the nitrosonium acceptor (LUMO). Therefore, for both the **1a**$-(NO^+)_2$ and **1b**$-(NO^+)_2$ species we calculated: (i) the atomic charges on the C_{ipso} (namely, QC_{ipso}) and C_{ortho} (namely, QC_{ortho}) aromatic carbons belonging to the flattened ring tightly close to NO^+, as well as the atomic charges on the nitrogen atom of the closer NO^+ cation (QN), and (ii) the energy of the HOMO (or next HOMO) and LUMO (or next LUMO) frontier orbitals involved in the cited contact (see Table 2), as well as the lobe expansion of such orbitals (Figure 5).

Clearly, in both of the geometries, the C_{ipso} aromatic carbons, bound to the methine bridge and belonging to the flattened aromatic ring placed between the couple of NO^+ cations, are favored to behave as the nucleophile. In fact, they are characterized, at the same time, by all the following three necessary conditions: (i) a tight contact with the nitrogen atom of NO^+, (ii) an appropriate negative atomic charge, and (iii) a good expansion of their orbital lobes within the HOMO. Indeed, although in both of the adduct geometries the C_{ortho} atoms have a negative charge greater than that of the C_{ipso} atoms, only on the first type of carbon is the relative expansion of the HOMO orbital lobes lacking (see Figure 5).

The data collected (see Table 2) confirmed a potential good propensity of both the three-body **1a**$-(NO^+)_2$ and **1b**$-(NO^+)_2$ adducts to undergo the electrophilic substitution by the NO^+ cation. However, although **1a**$-(NO^+)_2$ displays the most useful LUMO−HOMO gap and QN−QC_{ipso} charge difference, we can assume that **1b**$-(NO^+)_2$ is the only populated geometry capable of undergoing an electrophilic attack by the NO^+_{up} unit, as judged by both the LUMO−HOMO energy gap (1.3 eV by NO^+_{up} against 2.8 eV by NO^+_{down}) and the QN−QC_{ipso} charge difference (0.658 by NO^+_{up} against 0.442 by NO^+_{down}). Figure 5 shows satisfactory lobe expansion for the calculated HOMO−LUMO orbitals of **1b**$-(NO^+)_2$, which provide evidence of a C_{ipso}−nucleophile/NO^+_{up}−electrophile interaction.

The same kind of calculation was repeated for the two-body **1b**−NO^+ and **1c**−NO^+ adducts[18] (the first being more stable by 6.4 kcal mol^{-1}; see Table 2), as well as for the parent uncomplexed resorc[4]arene **1**. By inspection of the data obtained, it may be argued that, starting from the free resorcarene **1**, complexation of each further NO^+ unit leads to a progressive increment of the QN−QC_{ipso} charge difference

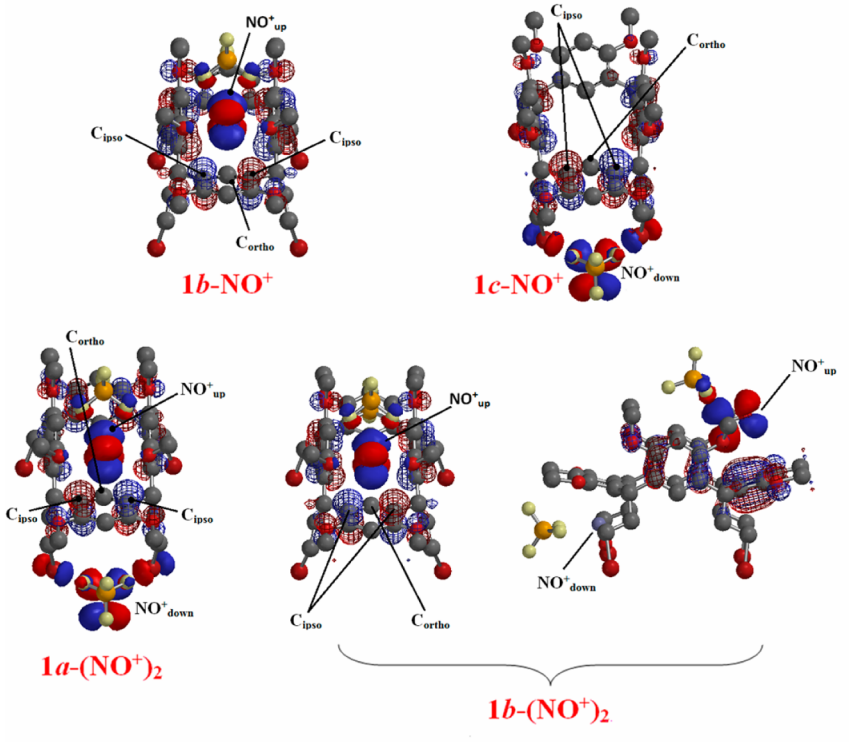

Figure 5. Lobe expansion calculated for the HOMO (mesh style) and LUMO (solid style) molecular orbitals of the two-body (**1b**−NO^+ and **1c**−NO^+) and three-body (**1a**$-(NO^+)_2$ and **1b**$-(NO^+)_2$) adducts.

dx.doi.org/10.1021/jo400489m | J. Org. Chem. 2013, 78, 6935−6946

Scheme 1. Plausible Chemical Evolution of Resorc[4]arene 1 Complexed as Three-Body 1b−$(NO^+)_2$ Adduct to Compound 4 after an Ipso-S_EAr by NO^+

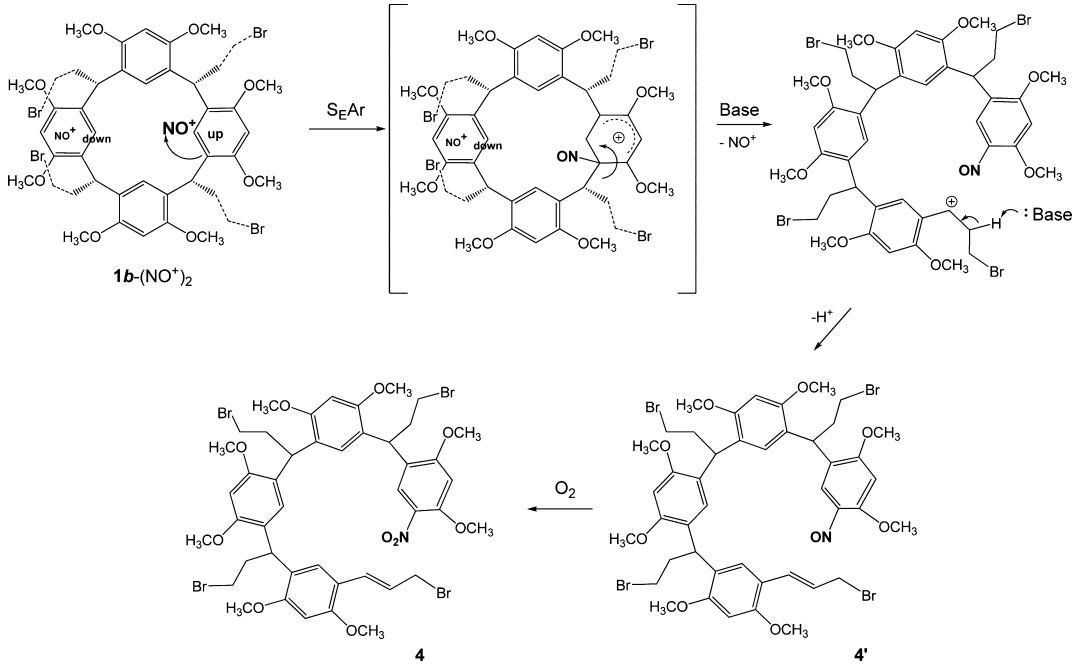

Scheme 2. Chemical Evolution of Olefin 4 to Aldehyde 5 after Addition of Water to the Reaction Mixture

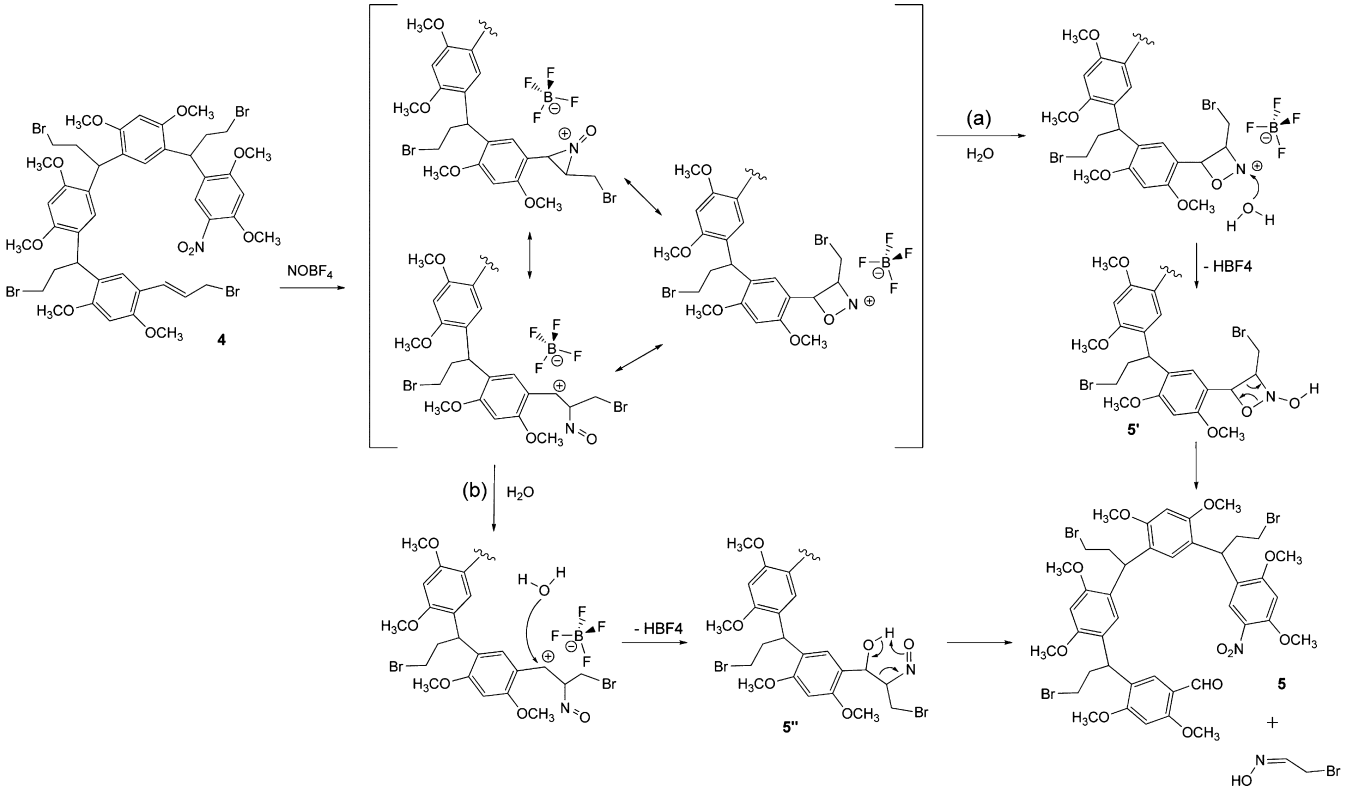

(from 0.292 to 0.649 electrons for the two-body adducts and to 0.661 electrons for the three-body adducts) and a decrease of the LUMO−HOMO energy gap (from 2.4 to 1.4 eV for the two-body adducts and to 1.3 eV for the three-body adducts), thus suggesting a potential increase in reactivity for the resulting complexes toward a C_{ipso} substitution.

Plausible Mechanistic Evolution of Resorc[4]arene 1 into Compounds 4 and 5. On the basis of the above-reported theoretical studies, the three-body **1b**−$(NO^+)_2$ geometry proved to be the prereactive supramolecular species. Thus, we may assume an ipso electrophilic attack on the resorcinol ring by NO^+_{up} (see Scheme 1), catalyzed by the second NO^+ unit located outside the macrocycle and leaning

dx.doi.org/10.1021/jo400489m | J. Org. Chem. 2013, 78, 6935−6946

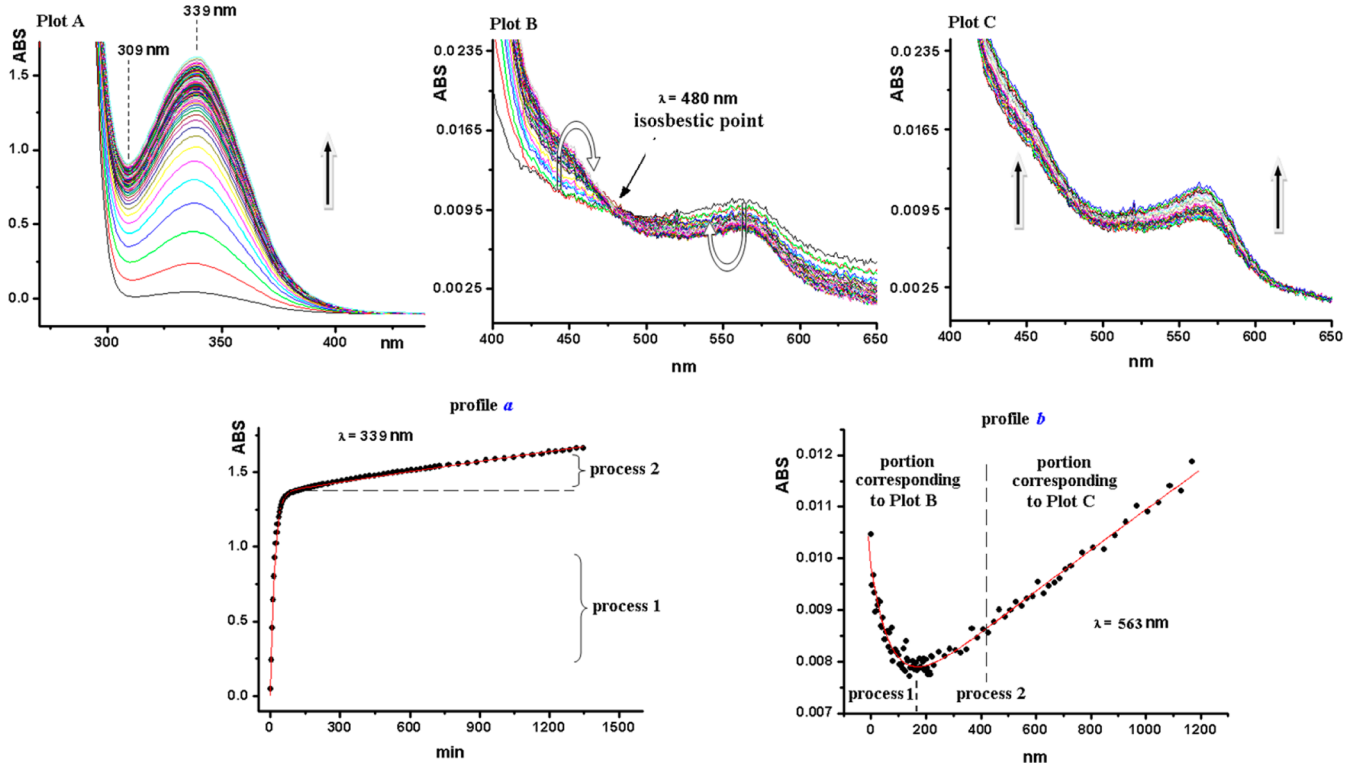

Figure 6. Kinetic pathway of the interaction between resorc[4]arene **2** and NO^+ monitored by UV spectroscopy at 339 and 563 nm. Plot A: growth of the spectral bands in the HEB zone; plot B: spectral evolution of the absorption bands in the LEB zone (registration window: from 0 to 408 min); plot C: spectral evolution of the absorption bands in the LEB zone (registration window: beyond 408 min).

against one aromatic ring (namely, NO^+_{down}). Displacement of the methine carbon from the Wheland intermediate, which leads to the ring-opening of macrocycle, yields a benzylic carbocation on the other side of the ruptured bond. Removal of the adjacent proton by a base provides alkene intermediate **4′**, which evolves to the final olefin **4** by spontaneous oxidation of NO to NO_2. Such an event happens even for temporary exposure to the air, as already shown for *p*-nitro-substituted phenols obtained from the corresponding *p*-nitroso compounds in the presence of oxygen.[23] Such a base-catalyzed mechanism was supported by the evidence that when the reaction was performed in the presence of 2,6-di-*tert*-butyl-4-methylpyridine (DBMP), it gave compound **4** in higher yield.

Taking into account the large excess of $NOBF_4$ used in the reaction and the well-known reactivity between nitrosonium cation and olefins,[24−26] a further progress of the reaction may be hypothesized (see Scheme 2), starting from olefin precursor **4** and leading to aldehyde **5** after addition of water, according to at least two possible mechanisms, namely a and b. With regard to mechanism a, the formation of intermediate **5′** as a precursor of the final aldehyde **5** finds a reasonable theoretical backing, because it was shown by high-level ab initio calculations that the four-membered cycle of the structure is more stable than the equivalent opened fragment.[27]

Mechanism b represents a more classic type of evolution, in which water attacks the benzylic carbocation (or its resonance structure consisting of a three-membered cycle, in analogy to bromonium) to afford intermediate **5″**, followed by a retro-aldol-like fragmentation. In both cases, however, the same final products would be formed, namely aldehyde **5** and the oxime derivative of 2-bromoethanal. DFT calculations (see the Supporting Information) indeed showed that mechanism b is the more likely pathway to aldehyde **5**.

A dedicated experiment on a simplified olefinic model compound treated with a 3-fold excess of $NOBF_4$ was devised (vide infra), which confirmed the supposed conversion of the olefinic double bond into the aldehyde group, with formation of the corresponding oxime. Moreover, these findings agreed with the above-mentioned process 2 monitored at λ = 313 nm (see Table 1), which belongs to the typical UV absorption range of carbonyl groups.

Kinetic Studies on Resorc[4]arene 2. The kinetic pathway for the formation of **2**−NO^+ complexes was monitored under pseudo-first-order conditions, recording in the 250−800 nm UV−visible wavelength range spectra of chloroform solutions containing a guest-to-host molar ratio of 10. By inspection of the overlapped UV−visible absorption profiles already shown in Figure 1 (bottom), it clearly results in a progressive and intense growth of two bands centered at 284 and 339 nm, in contrast with the visible zone, where all the bands show a very weak absorption (Figure 6, plot A). In fact, in the wavelength range from 500 to 600 nm, only electronic transitions seriously hampered by the high noise level may be observed and appeared only by a strong magnification of the spectra. Nevertheless, the existence of an isosbestic point centered at 480 nm (Figure 6, plot B) accounts for an interconversion process occurring between two species.

As already observed for resorc[4]arene **1**, also in this case the large excess of NO^+ cation used could account for the formation of isomeric complexes with stoichiometry greater than 1:1. However, comparison of the spectral changes observed over the time in the HEB and LEB zones for **1**−NO^+ and **2**−NO^+ complexes clearly showed a quite different

dx.doi.org/10.1021/jo400489m | J. Org. Chem. 2013, 78, 6935−6946

evolution rate of the corresponding processes (Figure 2S of the Supporting Information), as a result of the replacement of the bromine atom in resorc[4]arene **1** with the ester carbonyl group in host **2**. In particular, when the host was **2**, the differential absorbance change in the HEB region with respect to those in the LEB zone was much faster than when the host was **1**. This behavior seems to suggest that when the host is **1**, the spectral transformations are governed by a NO^+ cation guest located in the upper rim of the resorcarene host, whereas the opposite position of the guest (i.e., NO^+ in the lower rim) is responsible for the observed modifications when the host is **2**. Nonlinear curve fitting of the spectral changes collected as a function of time in the HEB zone (λ_{max} = 339 nm; see Table 1) led to the identification of two consecutive and reversible processes (Figure 6, profile a), both following first-order kinetics but featuring very different rates, the second one being much slower ($k_1 = 1.5 \times 10^{-6}$ s^{-1}) than the first one ($k_1 = 9.2 \times 10^{-4}$ s^{-1}). Equivalent findings were obtained by kinetic analysis performed at λ = 563 nm (Figure 6, profile b). However, in this case, the rate constant for the first process ($k_1 = 2.2 \times 10^{-4}$ s^{-1}) was found 4-fold lower than that registered in the HEB zone. Finally, as found for resorc[4]arene **1**, a drastic change in the trend was detected when the absorbance reached a minimum (portion corresponding to plot B in profile b), coincident with the step of the process responsible for the isosbestic point at λ = 480 nm. Thus, we can assume that, also in this case, process 1 leads to the formation of a prereactive supramolecular species able to undergo the chemical evolution described by the linear kinetic profile of process 2.

Resorc[4]arene **2** was subjected to the same experiments with $NOBF_4$ as those performed for resorc[4]arene **1**, featuring changes in the reaction time and in the [**2**]/[NO^+] molar ratio. Periodic monitoring of the reaction mixtures was carried out by both NMR and HPLC techniques, before and after the quenching of the chloroform solutions with water. When bleached solutions from [**2**]/[NO^+] mixtures in a 1:3 molar ratio were examined by NP-HPLC (Figure 3S of the Supporting Information), besides the parent resorc[4]arene **2** (peak A), a major peak (B, 70%) was present, whereas a second product (peak C) was reduced to trace levels. Compounds **6** and **7** (corresponding to peaks B and C, respectively) were first isolated by preparative TLC, checked for purity by NP-HPLC (85−90%), and then fully characterized by NMR and ESI-HRMS (see the Supporting Information).

Not surprisingly, resorc[4]arene **2**, which differs from resorc[4]arene **1** only in the nature of the side chains, gave rise to the same kind of products in the reaction with nitrosonium cation, although with different yields. In other words, the same typology of structures was assigned to the two products **6** and **7** recovered from the reaction (see Chart 3), i.e., **6** is a *trans*-olefin (two coupled protons at δ = 6.38 and 7.86 were detected, J = 16 Hz) and **7** contains an aldehyde group (singlet at δ = 10.25). To shed light on the possible mechanistic evolution of resorc[4]arene **2** to compounds **6** and **7**, we set up several experiments followed by classical molecular modeling calculations.

Molecular Modeling Studies on Resorc[4]arene 2. Three-body adducts of resorc[4]arene **2** with NO^+ were similarly built starting from **2b**−NO^+ and **2c**−NO^+ geometries obtained from previous studies on **2**−NO^+ complexes under conditions of host excess.[18] The adducts were modeled by adding a second NO^+ cation inside the cone cavity of the **2c**−NO^+ two-body adduct, considering also the presence of the

Chart 3. Structures of Compounds 6 and 7 Obtained from Resorc[4]arene 2

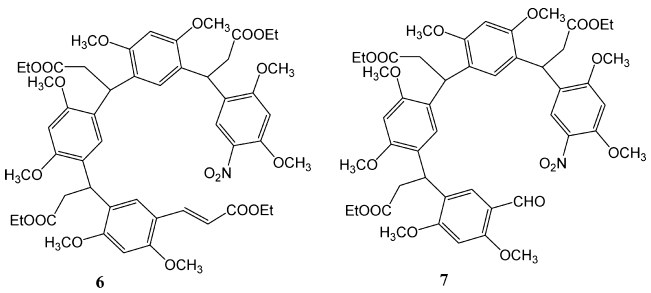

counterion (BF_4^-) to keep the supermolecules neutral. Two different geometries, namely **2a**−$(NO^+)_2$ and **2b**−$(NO^+)_2$, were obtained by insertion of NO^+ cation either upon the flattened ring overhanging the other NO^+ unit or at the top side of the other flattened ring. Afterward, the two geometries were fully optimized as described above (see Figure 7). The

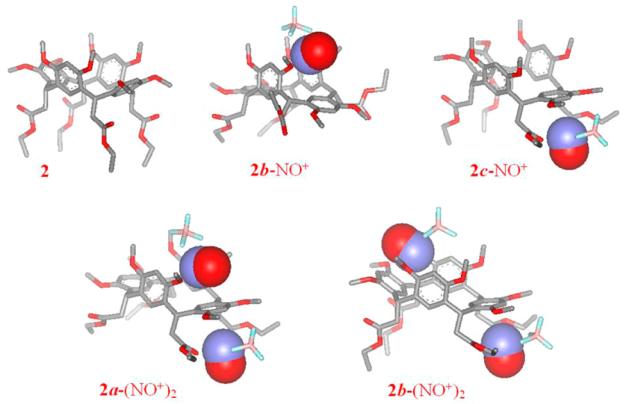

Figure 7. Structures obtained by DFT calculations for resorc[4]arene **2** and its two-body (**2b**−NO^+ and **2c**−NO^+) and three-body (**2a**−$(NO^+)_2$ and (**2b**−$(NO^+)_2$) adducts with NO^+ cation (the counterion BF_4^- was added to keep neutral the supermolecules).

corresponding data (i.e., energies of the HOMO (or next-HOMO) and LUMO (or next-LUMO) molecular orbitals as well as the atom charge located on the C_{ipso} and C_{ortho} aromatic carbons and on the nitrogen atom of the NO^+ units) are collected in Table 2. Geometry **2a**−$(NO^+)_2$ (0.0 kcal mol^{-1}, Boltzmann population in the gas phase 69.9% at 298 K) proved to be more stable than **2b**−$(NO^+)_2$ by 0.5 kcal mol^{-1} (Boltzmann population in the gas phase 30.1% at 298 K). As already found for resorc[4]arene **1**, the C_{ortho} aromatic carbons do not possess at the same time all the features necessary to behave as the nucleophile toward the tightly close NO^+ unit. As depicted in Figure 8, in fact, lobe expansion, that in the HOMO orbital should depart from the C_{ortho} atom, is missing.

Comparison of QN−QC_{ipso} charge differences for the two **2a**−$(NO^+)_2$ and **2b**−$(NO^+)_2$ geometries clearly shows that the **2a**−$(NO^+)_2$ adduct is the most favored to behave as the nucleophile toward the NO^+_{down} unit, for both energetic (greater Boltzmann population at 298 K) and electrostatic (greater QN−QC_{ipso} difference) factors (see Table 2). Notably, in this case, the LUMO−HOMO energy gap and the QN−QC_{ipso} charge differences provide evidence of a greater reactivity of the NO^+_{down} unit with respect to the NO^+_{up}. Moreover, also for resorcarene **2**, complexation of each further

dx.doi.org/10.1021/jo400489m | J. Org. Chem. 2013, 78, 6935−6946

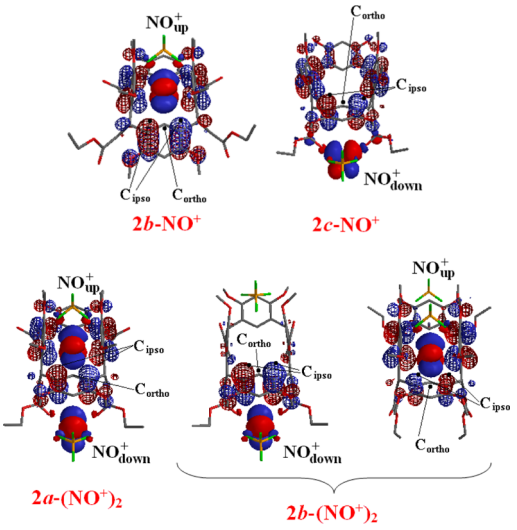

Figure 8. Lobe expansion calculated for the HOMO (mesh style) and LUMO (solid style) molecular orbitals of the two-body (**2b**−NO^+ and **2c**−NO^+) and three-body (**2a**−$(NO^+)_2$ and **2b**−$(NO^+)_2$) adducts.

NO^+ unit leads to a progressive increment of the QN−QC_{ipso} charge difference and a decrease in the LUMO−HOMO energy gap. In other words, progressive encapsulation of NO^+ units improves the nucleophilicity of the C_{ipso} carbon atoms and enables the macrocycle to undergo the electrophilic substitution. Such findings easily justify the lack of electrophilic reactivity that we observed[18] when [NO^+]/[**2**] molar ratios were ≤1.

Rationale for the Ipso Electrophilic Attack by NO^+ on Resorc[4]arene 2. On the basis of the above-reported theoretical studies, we can imagine the chemical evolution of resorc[4]arene **2** to compound **6** as the sum of two events: the first one allows the fast allocation of one NO^+ unit beside a flattened aromatic ring (i.e., NO^+_{down}) and corresponds to process 1 of Figure 6; the second one results from the electrophilic attack on a C_{ipso} carbon atom by the same NO^+_{down} unit, triggered by the quite fast insertion of a second NO^+ cation into the cone cavity (i.e., NO^+_{up}) and corresponds to process 2, monitored at both 339 and 563 nm. Most likely, such transformation takes place from the three-body **2a**−$(NO^+)_2$ prereactive species, whose formation is suggested by the isosbestic point detected at 480 nm (Figure 6, plot B). Notably, process 2 also describes the chemical evolution of olefin **6** to aldehyde **7** (see Chart 3), according to the same mechanism depicted in Scheme 2 for resorc[4]arene **1**. To confirm the mechanism of such conversion, already envisioned for resorc[4]arene **1** (vide supra), (*E*)-2,4-dimethoxycinnamic acid ethyl ester[28] was chosen as a simplified olefinic model and treated with a 3-fold excess of $NOBF_4$ salt (see Experimental Section for conditions). As expected, 2,4-dimethoxybenzaldehyde was recovered as main product (22% yield) after the quenching with water.

Notably, the rate constant for the **4** → **5** conversion (1.2×10^{-5} s^{-1}, see Table 1) was 8-fold greater than that for the **6** → **7** reaction (1.5×10^{-6} s^{-1}), thus accounting for the different relative amount of aldehydes **5** (34%) and **7** (2%) recovered by decomposition of intermediate olefins **4** and **6**, respectively, under the same reaction conditions. In fact, in the case of olefin **6**, the availability of the double bond π electrons is reduced by the presence of the electron-withdrawing ester carbonyl group in the α position, with respect to the bromoethyl function in compound **4**. According to these considerations, we treated olefin **6** with a 3-fold excess of $NOBF_4$ salt in chloroform for 24 h (see Experimental Section for conditions): after quenching with water, we isolated aldehyde **7** (30% yield), while partly recovering the starting material. The formation of aldehyde **7** as main product from olefin **6** also revealed the stability of the Ar−CH−Ar system in a linear arrangement toward NO^+ and thus the peculiarity of the reaction of tetracyclic resorcarenes **1** and **2** with excess added $NOBF_4$ salt. In particular, the results provide strong evidence of the key catalytic role of NO^+ in promoting the C_{ipso} aromatic substitution only when engaged in a convenient supramolecular arrangement with the resorcarene host.

CONCLUDING REMARKS

We investigated the interaction of resorc[4]arenes **1** and **2** in the cone conformation with $NOBF_4$ in chloroform solution. Under conditions of host-to-guest excess, we have already shown that the kinetic trend of the complexation is connected to the side-chain functionality of the host. Now, further experiments with guest-to-host excess revealed the formation of specific nitration products according to a postulated S_EAr mechanism. The main products **4** and **6** (from **1** and **2**, respectively) are derived from the rupture of one of the methine bridges that leads to the loss of the C_{4v} symmetry of the host conformation, via an ipso-substitution of a quaternary aromatic carbon. Although such reactivity is independent of the nature of the side chains, the overall yields of the reaction were somehow dependent on the substitution, the final oxidation products (aldehydes **5** and **7** from **4** and **6**, respectively) being preferentially formed in the case of the bromoethyl side chain (i.e., from olefin **4**).

As shown by molecular modeling and frontier orbital calculations, **1b**−$(NO^+)_2$ and **2a**−$(NO^+)_2$ three-body adducts are the prereactive supramolecular species capable of undergoing an electrophilic attack by the NO^+ cation: in the first case, it involves the NO^+_{up} unit, while for host **2** it is the NO^+_{down} unit to perform the attack. Such charge-transfer three-body adducts are an interesting example of supramolecular control of a reaction outcome.[17a,29] In particular, as critical precursors to an ipso-aromatic substitution, they provide strong evidence of the key catalytic role of NO^+ in promoting the reaction only when it is engaged in a convenient supramolecular arrangement with the resorcarene host. Such findings easily justify the lack of electrophilic reactivity previously observed under conditions of host excess.

EXPERIMENTAL SECTION

Calculation Procedures. All molecular modeling calculations were performed by use of the computer program SPARTAN 08 v 1.2.0 (Wave Function Inc., Irvine, CA). Structures of the three-body **1a**−$(NO^+)_2$, **1b**−$(NO^+)_2$, **2a**−$(NO^+)_2$, and **2b**−$(NO^+)_2$ adducts were obtained by insertion of a new NO^+ cation inside the cone cavity of the already modeled two-body **1c**−NO^+ and **2c**−NO^+ adducts,[18] respectively. As starting geometries of resorc[4]arenes **1** and **2** and of two-body **1b**−NO^+, **2b**−NO^+, and **2c**−NO^+ adducts were again used as the most relevant previously obtained.[18] Within the two-body and three-body adducts, the positive charge of each NO^+ cation has been counterbalanced by addition of an equivalent number of BF_4^- units, placed in close proximity. Afterward, all the structures were optimized at the Hartree−Fock (HF) 3-21G level of theory and then redefined by the DFT method, at the B3LYP/6-31G(d) level of theory. Natural atomic charges, as well as energies of the HOMO (and next HOMO)

dx.doi.org/10.1021/jo400489m | J. Org. Chem. 2013, 78, 6935−6946

and LUMO (and next LUMO) orbitals, were also calculated accordingly. DFT calculations were also performed on uncomplexed resorc[4]arenes **1** and **2** as well as on $NOBF_4$.

General Procedure for the Reaction of Resorc[4]arenes 1 and 2 with $NOBF_4$ Salt. Resorc[4]arenes **1** and **2** used as hosts were prepared as previously described.[18] Stock solutions of $NOBF_4$ salt (Aldrich) and resorc[4]arenes **1** and **2** (1×10^{-2} M) were prepared in freshly distilled HPLC grade chloroform under a nitrogen atmosphere in an isolated glovebox at room temperature. The two solutions were then mixed to reach [host]/[guest] molar ratios of 1:1, 1:2, and 1:3. After 24 h, the intensely colored 1:3 reaction mixtures were quenched with water several times, extracted with chloroform, and dried over Na_2SO_4. The bleaching was always accompanied by the disappearance of the dark blue or purple color and led to pale yellow solutions. HPLC was used to monitor the reactions (see the Supporting Information for chromatographic conditions) before and after quenching with water to get quantitative information on covalent nitration products **4**–**7**, which were isolated and purified with preparative TLC plates (eluent: chloroform for **4** and **5** and dichloromethane–hexane–ethyl acetate, 7:1.5:1.5 for **6** and **7**; 85–90% purity, checked by analytical NP-HPLC (see the Supporting Information for chromatographic conditions).

Compound 4. Pale yellow oil, 91.9 mg, 0.086 mmol (44% yield). ^1H and ^{13}C NMR signals are given in the Supporting Information. Anal. Calcd for $C_{44}H_{51}Br_4NO_{10}$: C, 49.23; H, 4.79; Br, 29.77; N, 1.30. Found C, 49.08; H, 4.77; Br, 29.69; N, 1.29. FT-IR (KBr): 2921, 2851, 1731, 1613, 1509, 1465, 1299 cm^{-1}.

Compound 5. Pale yellow oil, 65.0 mg, 0.066 mmol (34% yield). ^1H and ^{13}C NMR signals are given in the Supporting Information. ESI-HRMS (positive): $C_{42}H_{48}Br_3NO_{11}Na$ requires 1002.06752 (monoisotopic), *m/z* found 1002.06810 ($[M + Na]^+$). FT-IR (KBr): 2924, 2855, 1728, 1615, 1508, 1468, 1299 cm^{-1}.

Compound 6. Pale yellow oil, 174.0 mg, 0.176 mmol (83% yield). ^1H and ^{13}C NMR signals are given in the Supporting Information. ESI-HRMS (positive): $C_{52}H_{63}NO_{18}Na$ requires 1012.39428 (monoisotopic), *m/z* found 1012.39290 ($[M + Na]^+$). FT-IR (KBr): 2927, 2854, 1726, 1606, 1506, 1465, 1299 cm^{-1}.

Compound 7. Pale yellow oil, 3.9 mg, 0.004 mmol (2% yield). ^1H and ^{13}C NMR signals are given in the Supporting Information. ESI-HRMS (positive): $C_{48}H_{57}NO_{17}Na$ requires 942.35242 (monoisotopic), *m/z* found 942.35230 ($[M + Na]^+$). FT-IR (KBr): 2927, 2854, 1726, 1606, 1506, 1465, 1299 cm^{-1}.

Reaction of (*E*)-2,4-Dimethoxycinnamic Acid Ethyl Ester with $NOBF_4$ Salt. A dry chloroform solution (1×10^{-2} M) of (*E*)-2,4-dimethoxycinnamic acid ethyl ester, available from previous studies,[28] was reacted with 3 equiv of $NOBF_4$ salt under a nitrogen atmosphere into an isolated glovebox at room temperature. After 24 h, water was added and the mixture was extracted with chloroform and dried over Na_2SO_4. The crude extract was purified by silica gel column chromatography (hexane–chloroform–methanol, 7:3:0.1) to yield 2,4-dimethoxybenzaldehyde as the main product (15.5 mg, 0.093 mmol, 22% yield). White powder (mp: 68–70 °C, lit.[30] 70–71 °C). ^1H NMR ($CDCl_3$, 400 MHz): δ (ppm) 10.26 (s, 1H, CHO), 7.78 (d, J = 8.67 Hz, 1H), 6.58 (dd, J = 8.7, 2.1 Hz, 1H), 6.47 (d, J = 2.1 Hz, 1H), 3.88 (s, 3H, OCH_3), 3.85 (s, 3H, OCH_3). ^{13}C NMR ($CDCl_3$, 75 MHz): δ (ppm) 188.3 (CHO), 166.2 (Ar–C4), 163.7 (Ar-C2), 130.7 (Ar-CH), 119.1 (Ar-C1), 105.8 (Ar-CH), 98.0 (Ar-CH), 55.6 (2 × OCH_3). ESI-HRMS (positive): *m/z* found 167.07010 ($[M + H]^+$), $C_9H_{11}O_3$ requires 167.07082 (monoisotopic mass). FT-IR (KBr): 1670, 1475, 1334, 1024 cm^{-1}.

Reaction of Compound 6 with $NOBF_4$ Salt. A dry chloroform solution (1×10^{-2} M) of compound **6** was reacted with 3 equiv of $NOBF_4$ salt under a nitrogen atmosphere into an isolated glovebox at room temperature. After 24 h, water was added and the mixture was extracted with chloroform and dried over Na_2SO_4. The crude extract was purified by silica gel column chromatography (dichloromethane–hexane–ethyl acetate, 7:1.5:1.5) to yield compound **7** as the main product (27.9 mg, 0.030 mmol, 30% yield).

■ ASSOCIATED CONTENT

Supporting Information

General experimental methods and spectroscopic characterization of compounds **4**–**7**. Cartesian coordinates of structures optimized at the B3LYP/6-31G(d) level of theory. This material is available free of charge via the Internet at http://pubs.acs.org.

■ AUTHOR INFORMATION

Corresponding Author

*Phone: +39-06-49912784. Fax +39-06-49912780. E-mail: ilaria.dacquarica@uniroma1.it (I.D.); marco.pierini@uniroma1.it (M.P.).

Present Address

‡Institut de Recerca Biomèdica (IRB-PCB), Barcelona, Spain.

Notes

The authors declare no competing financial interest.

■ ACKNOWLEDGMENTS

We acknowledge financial support from Center for Life NanoScience@LaSapienza, Istituto Italiano di Tecnologia (IIT), Roma, Italy (Funds 2011–2015) and Sapienza Università di Roma, Italy (Funds for Selected Research Topics 2011–2013). We gratefully acknowledge Dr. Deborah Quaglio for her technical assistance.

■ REFERENCES

(1) Wang, P. G.; Xian, M.; Tang, X.; Wu, X.; Wen, Z.; Cai, T.; Janczuk, A. J. *Chem. Rev.* **2002**, *102*, 1091–1134.

(2) Megson, I. I.; Webb, D. J. *Expert Opin. Invest. Drugs* **2002**, *11*, 587–601.

(3) Granik, V. G.; Grigor'ev, N. B. *Russ. Chem. Bull.* **2002**, *51*, 1375–1422.

(4) Thatcher, G. R. J.; Weldon, H. *Chem. Soc. Rev.* **1998**, *27*, 331–337.

(5) Wallace, J. L.; Miller, M. J. S. *Gastroenterology* **2000**, *119*, 512–520.

(6) Kirsch, M.; Korth, H.-G.; Sustmann, R.; de Groot, H. *Biol. Chem.* **2002**, *383*, 389–399.

(7) Mirvish, S. S. *Cancer Lett.* **1995**, *93*, 17–48.

(8) Hoffman, D.; Hoffman, I.; El-Bayoumy, K. *Chem. Res. Toxicol.* **2001**, *14*, 767–790.

(9) Espey, M. G.; Miranda, K. M.; Thomas, D. D.; Wink, D. A. *J. Biol. Chem.* **2001**, *276*, 30085–30091.

(10) (a) Hayton, T. W.; Legzdins, P.; Sharp, W. B. *Chem. Rev.* **2002**, *102*, 935–992. (b) Sellmann, D.; Blum, N.; Heinemann, F. W.; Hess, B. A. *Chem.—Eur. J.* **2001**, *7*, 1874–1880. (c) Gaviglio, C.; Ben-David, Y.; Shimon, L. J. W.; Doctorovich, F.; Milstein, D. *Organometallics* **2009**, *28*, 1917–1926. (d) Chan, S.-C.; Pat, P.-K.; Lau, T.-C.; Wong, C.-Y. *Organometallics* **2011**, *30*, 1311–1314.

(11) Rathore, R.; Lindeman, S. V.; Rao, K. S. S. P.; Sun, D.; Kochi, J. K. *Angew. Chem., Int. Ed.* **2000**, *39*, 2123–2127.

(12) Zyryanov, G. V.; Kang, Y.; Stampp, S. P.; Rudkevich, D. M. *Chem. Commun.* **2002**, 2792–2793.

(13) Zyryanov, G. V.; Kang, Y.; Rudkevich, D. M. *J. Am. Chem. Soc.* **2003**, *125*, 2997–3007.

(14) Rudkevich, D. M. *Angew. Chem., Int. Ed.* **2004**, *43*, 558–571.

(15) Rathore, R.; Abdelwahed, S. H.; Guzei, I. A. *J. Am. Chem. Soc.* **2004**, *126*, 13582–13583.

(16) (a) Rudkevich, D. M.; Kang, Y.; Leontiev, A. V.; Organo, V. G.; Zyryanov, G. V. *Supramol. Chem.* **2005**, *17*, 93–99. (b) Wanigasekara, E.; Leontiev, A. V.; Organo, V. G.; Rudkevich, D. M. *Eur. J. Org. Chem.* **2007**, 2254–2256.

(17) (a) Wanigasekara, E.; Gaeta, C.; Neri, P.; Rudkevich, D. M. *Org. Lett.* **2008**, *10*, 1263−1266. (b) Hines, J. H.; Wanigasekara, E.; Rudkevich, D. M.; Rogers, R. D. *J. Mater. Chem.* **2008**, *18*, 4050−4055.
(18) Botta, B.; D'Acquarica, I.; Delle Monache, G.; Nevola, L.; Tullo, D.; Ugozzoli, F.; Pierini, M. *J. Am. Chem. Soc.* **2007**, *129*, 11202−11212.
(19) (a) Borodkin, G. I.; Elanov, I. R.; Andreev, R. V.; Shakirov, M. M.; Shubin, V. G. *Russ. J. Org. Chem.* **2006**, *42*, 406−411. (b) Kim, E. K.; Kochi, J. K. *J. Org. Chem.* **1989**, *54*, 1692−1702.
(20) Högberg, A. G. S. *J. Am. Chem. Soc.* **1980**, *102*, 6046−6050 and references cited therein..
(21) (a) Modro, T. A.; Yates, K. *J. Am. Chem. Soc.* **1976**, *98*, 4247−4250. (b) Sankararaman, S.; Haney, W. A.; Kochi, J. K. *J. Am. Chem. Soc.* **1987**, *109*, 5235−5249. (c) Masnovi, J. M.; Sankararaman, S.; Kochi, J. K. *J. Am. Chem. Soc.* **1989**, *111*, 2263−2276.
(22) Bosch, E.; Kochi, J. K. *J. Org. Chem.* **1994**, *59*, 3314−3325.
(23) Böhmer, V. In *The Chemistry of Phenols*; Rappoport, Z., Ed.; Wiley: Chichester, UK, 2003; Chapter 9, p 639, and references cited therein.
(24) Borodkin, G. I.; Elanov, I. R.; Podryvanov, V. A.; Shakirov, M. M.; Shubin, V. G. *J. Am. Chem. Soc.* **1995**, *117*, 12863−12864.
(25) Bosch, E.; Kochi, J. K. *Res. Chem. Intermed.* **1996**, *22*, 209−224.
(26) Zyk, N. V.; Nesterov, E. E.; Khlobystov, A. N.; Zefirov, N. S.; Barnhurst, L. A.; Kutateladze, A. G. *J. Org. Chem.* **1999**, *64*, 7121−7128.
(27) Borodkin, G. I.; Shubin, V. G. *Russ. Chem. Rev.* **2001**, *70*, 211−230.
(28) Botta, B.; Di Giovanni, M. C.; Delle Monache, G.; De Rosa, M. C.; Gács-Baitz, E.; Botta, M.; Corelli, F.; Tafi, A.; Santini, A.; Benedetti, E.; Pedone, C.; Misiti, D. *J. Org. Chem.* **1994**, *59*, 1532−1541.
(29) (a) Maia, A.; Landini, D.; Penso, M.; Brandt, K.; Siwy, M.; Schroeder, G.; Gierczyk, B. *New J. Chem.* **2001**, *25*, 1078−1083. (b) Chen, J.; Rebek, J., Jr. *Org. Lett.* **2002**, *4*, 327−329. (c) Iwasawa, T.; Mann, E.; Rebek, J., Jr. *J. Am. Chem. Soc.* **2006**, *128*, 9308−9309. (d) Rosokha, S. V.; Kochi, J. K. *J. Org. Chem.* **2002**, *67*, 1727−1737.
(30) Smith, R. A. J.; Bin Manas, A. R. *Synthesis* **1984**, 166−168.